Chapter

Optical Waveguides Based on Sol-Gel Coatings

Helena Cristina Vasconcelos

Abstract

This chapter focuses on developing coatings for use as waveguides for integrated optics and photonics. Thin (or thick) films of silica-based inorganic materials and organic-inorganic hybrids can be easily obtained using the sol-gel and spin-coating method, followed by rapid thermal annealing to obtain dense films of good optical quality. The waveguide thermal, structural, and optical properties can be characterized using differential thermal analysis, X-ray diffraction, Fourier-transform infrared spectroscopy, Raman spectroscopy, scanning electron microscopy, and atomic force microscopy. Waveguides can be both doped with semiconductor microcrystallites and rare-earths for the development of optical devices, where light is confined to one or two dimensions (planar, channel or strip loaded).

Keywords: sol-gel, optical waveguides, coatings, spin-coating, silica, rare-earths, semiconductor microcrystallites

1. Introduction

The optical technology enables larger bandwidth over larger distances at enhanced power efficiency as compared to the use of electrical connections. In practice, this is based on the hybrid integration in one single substrate of many small individual components connected to each other by optical waveguides, an approach known as integrated optics (IO) (e.g., bring together on a single platform, filters, lenses, modulators, beam splitters, amplifiers, lasers, photodetectors, etc.). The basic idea behind IO is the management of light by waveguides and not by free space optical components like lenses and mirrors. Moreover, the success achieved in the long-distance transmission fiber in the 1960s has increased the attention toward the optical waveguides. Anderson, in 1965, used planar waveguides and optical circuit components for applications in the near infrared (IR) [1]. Later, in 1969, was first reported an experimental application of prims-film coupler and Miller first introduced the term IO [2]. Light can therefore be guided and confined by dielectric waveguides, such as those made of glass (SiO_2) deposited on quite a large number of substrates, but mainly silicon. The large waveguide cross-section allows easy coupling with optical fibers. Other hi-tech characteristics are their larger bandwidth, low energy requirements, and immunity to electromagnetic interference. Optical waveguides are thus the basic elements for confinement and transmission of light over various distances, ranging from a few μm, in IO, to several kilometers, in the transmission of optical fibers over long distances.

The increasing use of optical communications, signal processing, and the development of new materials has created important advances in IO. The efficient use of the bandwidth offered by optical fibers also contributed to the success of this technology. The optical waveguides can be made of different materials. Each material has its own advantages and disadvantages. Therefore, the choice of a material to develop a new optical waveguide is usually the result of certain commitments. For example, considerable effort has been made to allow optical integration entirely using semiconductor materials (for example, GaAs/GaAlAs and InP/InGaAsP). However, its manufacture is not an easy task and requires complex epitaxial growth, usually by liquid phase epitaxy or metal-organic vapor epitaxy growth techniques. Unfortunately, these techniques do not offer the necessary manufacturing speed or the thicknesses required for the normal set-up of optical waveguides. Therefore, the use of glass (amorphous materials) has become widespread to develop planar waveguides (or slabs), as well as rapid deposition techniques (e.g., immersion or rotation of solutions to get glass by the sol-gel process). The sol-gel process has become a feasible method for fabricating thick films of desired composition to be carried out at speeds closer to those required in large-scale production. In addition, the use of silicon as a substrate also has numerous advantages due to the layout of silica-on-silicon (SiO_2/Si), one of the most important technologies in OI.

The arrival of low-loss silica fibers, whose refractive index perfectly matches the glass waveguides, contributed to making this material one of the most widely used in IO [3]. Currently, the sol-gel process offers great versatility because of the ease to functionalizing the glass structure with a wide variety of dopants. In fact, to provide all optical functions, from passive waveguides, electrical-driven modulators and switches, optical pumped active waveguides, optical-driven modulators and switches, and optical nonlinear devices, both optically active and optically nonlinear materials are needed. These materials can be respectively provided by two types of dopants: lasing species, such as rare-earths (RE) ions and semiconductor microcrystals. Hence, doping glass waveguides with Er^{3+} or Nd^{3+} ions allows glass to act as optical amplifier, while nonlinear properties can be introduced to silicate glasses by doping with semiconductor microcrystals and thus allowing to explore the Kerr effect [4]. Therefore, glasses can be used as optical waveguides, combining dielectric properties and providing specific functional responses for two main applications: as optical communication devices [5] and sensors [6].

2. Optical planar waveguides

A slab waveguide is similar to an optical fiber, except that it is in planar shape rather than cylindrical waveguide, where a low refractive index substrate contains on its surface a slab (or channel) of higher index material, along which light is guided by total internal reflection. The guiding material should also allow the linear and nonlinear optical properties to be varied in a straightforward way, over a wide range.

2.1 Linear dielectric waveguides

The most common structure of a dielectric waveguide is shown in **Figure 1**, which is made of three overlapping layers of dielectric materials [7]. The first layer (which is usually referred as the substrate) and the third layer (also named cladding) are both semi-infinite and have refractive indices n_1 and n_3, respectively, while the layer on the middle (guiding layer or core) has thickness d, and refractive

index n_2. In order to ensure total internal reflection at each interface $n_2 > n_1$ and $n_2 > n_3$. It is illuminated at one end by a monochromatic light source.

A waveguide as shown in **Figure 1** can be made by depositing a high-index guiding layer onto a flat substrate were the cladding can be the air. Because of this asymmetric geometry, since $n_2 > n_1 > n_3$, this kind of waveguide is often described as an asymmetric slab waveguide (**Figure 1a**). However, if $n_1 = n_3$, the waveguide is symmetric (**Figure 1b**). Light is confined by the total internal reflection at the substrate and layer cladding interfaces; and the phenomenon can be analyzed by the ray optics approach. The ray of light experiencing successive total internal

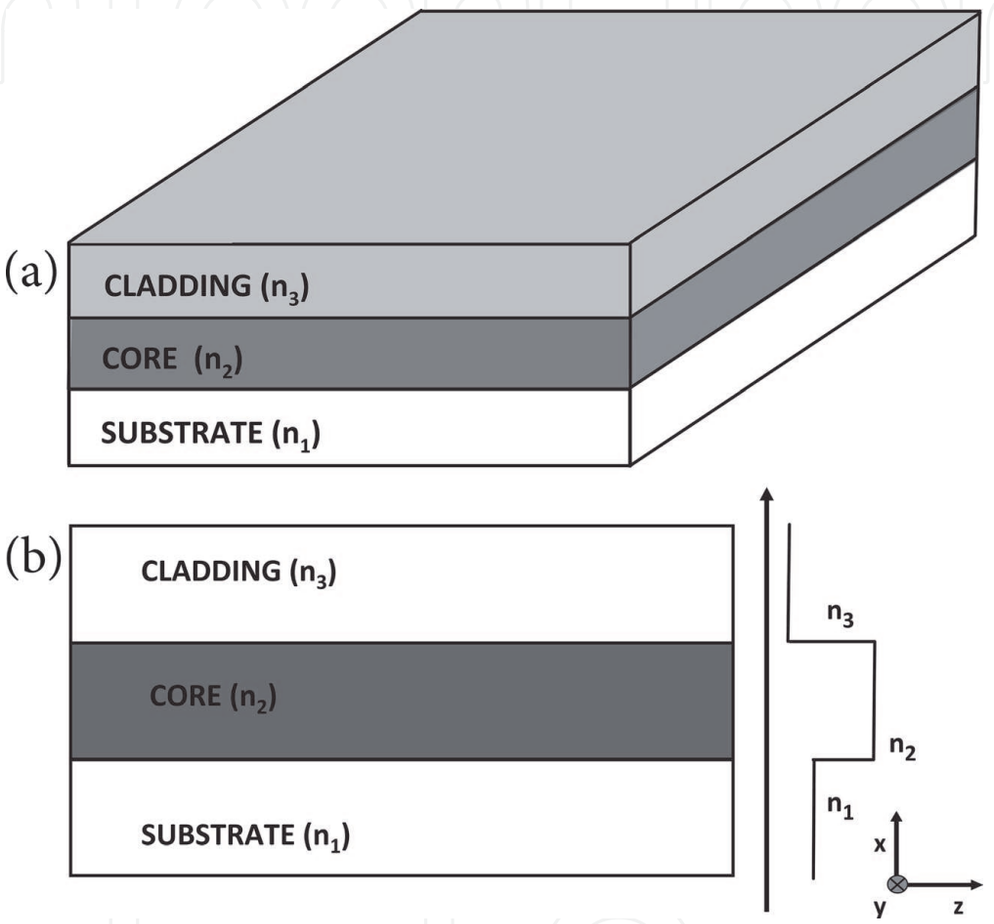

Figure 1.
Geometry of (a) an asymmetric slab waveguide ($n_2 > n_1 > n_3$), and (b) asymmetric slab waveguide with its refractive index profile.

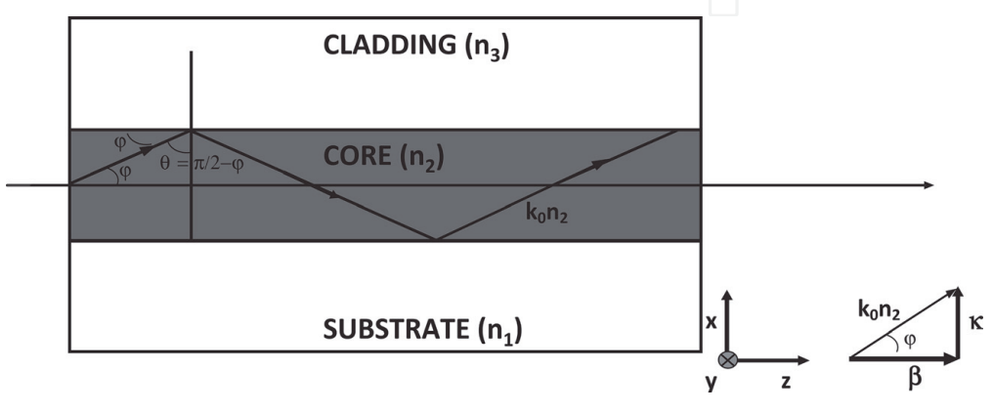

Figure 2.
Asymmetric slab waveguide with a propagating light ray in its core and geometric (vectorial) relationship between the propagation constants of dielectric waveguide.

reflections at the main interfaces will propagate continually along the central layer without loss [7]. This happens if the incident angle is small enough.

The propagation of signal within the guiding layer of planar waveguide is shown in **Figure 2**, where k_0 is the plane wave propagation constant in free space (or free-space wavenumber). The free-space wavenumber can be expressed as a function of frequency and velocity, or the wavelength:

$$k_0 = \frac{\omega}{c} = \frac{2\pi f}{c} = \frac{2\pi}{\lambda} \tag{1}$$

From geometric optics, it is known that a ray of light will follow Snell's law while crossing the interfaces of the core with the two surrounding layers. In view of **Figure 2**, the condition for total internal reflection is given by [8]:

$$\sin^{-1}\left(\frac{n_1}{n_2}\right) < \theta < \sin^{-1}\left(\frac{n_3}{n_2}\right) \tag{2}$$

The light ray is traveling in the z-direction of an optically isotropic medium with constant internal reflection at the core-cladding interface (2–3) and the core-substrate interface (2–1). The ray must interfere constructively with itself to propagate successfully. Otherwise destructive interference will destroy the wave. The theory and equations of dielectric waveguide can be found in the literature [9]. However, here it is briefly highlighted just a few important mode equations. Assuming a TE polarization (electric field polarized in the z-direction), the propagation constants along z (longitudinal direction) and x (transverse direction) are, respectively, β and κ, giving by:

$$\beta = k_0 n_2 \cos\varphi \tag{3}$$

$$\kappa = k_0 n_2 \sin\varphi \tag{4}$$

At each interface, the light ray that undergoes total reflection suffers phase shifts, ϕ_{2-3} and ϕ_{2-1}, respectively, at the cladding and substrate, which depend on the refractive indices of the three layers (1, 2, and 3), and are equal to:

$$\phi_{2-3} = -2\tan^{-1}\left(\frac{\left(n_2^2\cos^2\varphi - n_3^2\right)^{\frac{1}{2}}}{n_2\sin\varphi}\right) = -2\tan^{-1}\left(\frac{\delta}{\kappa}\right) \tag{5}$$

$$\phi_{2-1} = -2\tan^{-1}\left(\frac{\left(n_2^2\cos^2\varphi - n_1^2\right)^{\frac{1}{2}}}{n_2\sin\varphi}\right) = -2\tan^{-1}\left(\frac{\gamma}{\kappa}\right) \tag{6}$$

where

$$\delta = \left(\beta^2 - k_0^2 n_3^2\right)^{1/2} \tag{7}$$

$$\gamma = \left(\beta^2 - k_0^2 n_1^2\right)^{1/2} \tag{8}$$

$$\kappa = \left(k_0^2 n_2^2 - \beta^2\right)^{1/2} \tag{9}$$

The phases $-2\phi_{2\text{-}3}$ and $-2\phi_{2\text{-}1}$, represent the Goos-Hänchen shifts [10]. From the solution of Maxwell's equations, it can be demonstrated that only certain discrete values of β are allowed [11]. Therefore, there are only a limited number of guided modes and the condition for being a guided mode is that β must be within two limits (up and down):

$$k_0 n_1 < \beta < k_0 n_2 \tag{10}$$

To avoid destructive interference as the light travel through the guide, the total phase shift for a ray that travels from the 2-3 interface to the 2-1 interface and back again must be a multiple of 2π. This leads to the condition [12]:

$$2k_0 n_2 d \sin\varphi - 2\phi_{2-3} - 2\phi_{2-1} = 2m\pi \tag{11}$$

where d is the thickness of the core (layer 2) and m is the mode number, which is a positive integer (0, 1, 2, ...). The fundamental mode corresponds to m = 0 and also to the lowest thickness ($d_{\min}$) of the waveguide. In other words, for the fundamental TE mode to be supported by a planar waveguide, the thickness of the waveguide must by equal or larger than $d_{\min}$. The dispersion relation for the slab waveguide [7] (or eigenvalue equation of the TE fundamental mode supported by the waveguide) is given by:

$$\tan(d\kappa) = \frac{\kappa(\delta+\gamma)}{\kappa^2 - \gamma\delta} \tag{12}$$

From Eq. (11), it is possible to obtain the minimum thickness for an asymmetric planar slab waveguide, which is given by:

$$d_{min} = \kappa^{-1}\left(\tan^{-1}\frac{\kappa(\delta+\gamma)}{\kappa^2 - \gamma\delta}\right) \tag{13}$$

From Eq. (9), if $\beta \rightarrow k_0 n_2$ (up limit), then k = 0 (as shown by the vectorial relationship of **Figure 2**), which correspond at the cut-off of the mode. Thus, in this situation, the waveguide thickness tends to infinite. In practical situations, this means that the waveguide thickness would become very large. Otherwise, if $\beta \rightarrow k_0 n_1$ (lower limit), then γ = 0 as shown by Eq. (8). Therefore, Eqs. (7) and (9) can be rewritten, respectively as:

$$\delta = k_0\left(n_1^2 - n_3^2\right)^{1/2} \tag{14}$$

$$\kappa = k_0\left(n_2^2 - n_1^2\right)^{1/2} \tag{15}$$

Substituting both Eqs. (14) and (15) in Eq. (13), after some rearrangement, it is then obtained the waveguide minimum thickness for asymmetric case:

$$d_{min} = \frac{\tan^{-1}\left(\left(n_1^2 - n_3^2\right)/\left(n_2^2 - n_1^2\right)\right)^{1/2}}{k_0\left(n_2^2 - n_1^2\right)^{1/2}} \tag{16}$$

For a single-mode operation at 1.5 μm wavelength, a guiding film with a refractive index equal to 1.52, deposited onto a silica glass substrate (n_1 = 1.46) surrounding by air (n_3 = 1), should have a thickness higher than 670 nm. Since the guide is asymmetric, then the maximum wavelength that can be guided to a guide layer thickness $d > d_{min}$ is given by [13]:

$$\lambda_{max} = \frac{2\pi d\left(n_2^2 - n_1^2\right)^{1/2}}{\tan^{-1}\left(\left(n_1^2 - n_3^2\right)/\left(n_2^2 - n_1^2\right)\right)^{1/2}} \tag{17}$$

This applies to transverse electric (TE) polarization, but a similar condition applies to transverse magnetic (TM) polarization [13]. Because of the absence of cut-off, symmetric waveguides ($n_1 = n_3$) permit the propagation of the guiding mode in a layer of very small thickness. In addition, symmetric waveguides need a cover layer of similar refractive index to that of the substrate. The cover layer serves as the protective cladding for the gain layer. The presence of the cover layer also increases the confinement factor of the guiding modes [9], resulting in reduced modal loss and hence pump threshold reduction.

The typical way to achieve modal analysis in a planar optical waveguide is by means of *m*-line spectroscopy, by a prism coupler, where light is introduced into a waveguide by means of evanescent wave coupling through a high index prism of a material.

However, there are three major mechanisms of losses in waveguides, and thereby the energy of guided modes is often attenuated by losses due to mechanisms of absorption (owing to photons destruction in materials), radiation (owing to waveguide bending or curvatures), and scattering (owing to surface roughness) [11]. Absorption loss is mainly due to material contaminations while scattering loss in dielectric planar waveguides is due in part by internal defects such as pores or crystalline defects, but mainly to surface roughness. Rayleigh and Mie scattering are the principal mechanisms of scattering loss and are both linear occurrences since they do not change the wavelength of the scattered light (contrary to what happens in the non-linear scattering caused by Raman and Brillouin mechanisms). Rayleigh scattering is inherent to glass and amorphous materials and is caused by the lack of homogeneity of the refractive index over small distances when compared to the wavelength of light. On the other hand, Mie's dispersion is due to the presence of defects and occurs at distances of the order of magnitude of the wavelength of the input light [11].

2.2 Nonlinear optics

Whenever a beam of light (of low intensity) propagates through a dielectric material, the nuclei and associated electrons of the atoms in the material form electric dipoles which oscillate at the same frequency as the incident beam, thus giving a linear relation between the polarization density and the electric field, $P = \varepsilon_0 \chi E$, where ε_0 is the permittivity of free space and χ is the electric susceptibility of the material [4]. For high intensity light, such as laser light, the amplitude of response of the atoms is no longer linear. Therefore, to the polarization density should be added higher order nonlinear terms and P represented as a power series expansion of the applied electric field E of the light:

$$P = \varepsilon_0 \left(\chi^{(1)} E^1 + \chi^{(2)} E^2 + \chi^{(3)} E^3 + \chi^{(4)} E^4 + \ldots \right. \tag{18}$$

were $\chi^{(1)}$, $\chi^{(2)}$, and $\chi^{(3)}$ are, respectively, the linear, second order and third-order susceptibilities. In *centrosymmetric* materials, the second order susceptibility is however absent, $\chi^{(2)} = 0$, and so the lowest order nonlinearity is the third-order:

$$P_{nl} = \varepsilon_0 \chi^{(3)} E^3 \tag{19}$$

P_{nl} become the dominant nonlinear component in Eq. (18). Due to $\chi^{(3)}$ nonlinearity, the pump wave generates a nonlinear polarization (output wave) which oscillates at frequency three times higher than the input frequency. The optical nonlinearity $\chi^{(3)}$ is a tensor with various coefficients being associated with

various effects, including the Kerr susceptibility $\chi^{(3)}$ (3ω). The Kerr effect is the intensity dependence of refractive index, which can be expressed by a nonlinear index coefficient n_2 (the Kerr coefficient) proportional to $\chi^{(3)}$. Thus, the total index n is given by:

$$n = n_0 + n_2 I \tag{20}$$

where n_0 is the linear refractive index and I is the optical intensity in W/cm^2 (thus n_2 will have units of cm^2/W).

Nonlinear optical materials are needed for communications components [14]. The knowledge of the nonlinear refractive index n_2 is essential to the analysis and use of nonlinear devices. While silica glass has exceptional optical characteristics for waveguide proposes, they very low nonlinear coefficient turn it in a material unsuitable for nonlinear applications. However, strong nonlinearities responses can be obtained by the addition of, for example, semiconductor microcrystallites to the silica host. What give to these microcrystals such capacity is that the nonlinear effects can be significantly enhanced compared with those of the bulk semiconductors. Hence, when the size of the microcrystallites decreases to nanometric sizes, its electronic properties start to change from bulk state properties to that of a quantum dot state [15]. The essential change is that of the increase of excitonic level relative to that of bulk semiconductor (blue shift) as the radius of microcrystallites semiconductor is reduced. Band-filling models have been successfully used to explain the maximum enhancement for crystal sizes in the vicinity of the excitonic Bohr radius (∼10–20 Å) [15]. For smaller crystals, size quantization effects dominate and the electron-hole Coulomb attraction becomes insignificant.

3. Sol-gel process for the fabrication of waveguides

Glasses are suitable materials for application of passive, active, and nonlinear optical devices, due to their characteristic physical and chemical properties, in particular their optical features, such as exceptional transparency and high threshold to optical damage. In particular, silica glasses are very attractive because they match perfectly with the optical fibers and thus present small coupling losses; high thermal, chemical, and mechanical stability. Moreover, silica glass exhibits very low expansion coefficient over silicon which allows the deposition of thick buffer films without failure, which is a crucial feature layer on silicon for waveguide proposes. Of particular importance in the field of photonic glasses is the SiO_2/Si technology, where silica glass-based waveguides can be fabricated using several techniques. Flame hydrolysis deposition (FHD) and chemical vapor deposition (CVD) provide excellent quality thin films and have been extensively investigated [16, 17]. An alternative approach to these production methods is the sol-gel process, which offers many advantages in terms of avoiding complex equipment and high cost procedures [18].

3.1 Sol-gel process to produce glass and ceramic materials

The sol-gel process is a method for producing glass and ceramic materials by low temperature polymerization reactions based on hydrolysis and condensation of alkoxides, whose general formula is $M(OR)_n$, where M is a metal atom and R is one alkyl group that allow to make various glassy materials with remarkable optical or photonic properties. This process allows the preparation of high-purity and homogeneous materials and results in the preparation of different kinds of shapes, like

bulk solids, fibers, film waveguides, and coatings for device applications with a great diversity in material composition and structures which is important for control of the functionality of IO devices [19]. The main advantage of sol-gel process is that of allowing thin film deposition, providing a great versatility in the development of devices with special optical functions, particularly materials with a strict chemical control of the processing parameters. This flexibility allows diverse modifications to the host glass and the addition of a wide variety of dopants, thus greatly increasing the range of functions and applications of the resulting components. In the fabrication of sol-gel waveguides, a careful control from the beginning of the process is required in order to enhance the properties of these devices, starting from a suitable choice of the chemical precursors up to a correct final annealing. Through the control of the viscosity of the deposition solution, different coating processes like dipping, spraying, and spinning can be used. The strict chemical control and high purity of the starting reagents, mixed in the liquid state, lead to homogenous gels with low impurity levels, which is especially adequate for photonic technologies.

Dopants in the form of salts or alkoxides can be added to the precursor solution (sol) in order to prepare doped photonic inorganic materials. However, a limitation for application of sol-gel materials into optical devices is the drawback imposed by the maximum achievable crack-free sol-gel glass thickness [20]. SiO_2/Si technology compatible with single mode fiber for 1.55 μm, the most widely used wavelength in optical communication, requires waveguides typically greater than 1 μm in thickness and thus the need to employ a multistep deposition procedure (each layer being 150 to ~300 nm thick). To overcome this obstacle, rapid thermal annealing has been used to fabricate films through the deposition of iterative cycles of deposition, achieving the total required thickness [21].

Almost all of the sol-gel planar waveguides are fabricated on asymmetric structure with a substrate of silica glass (or a silicon with a buffer layer) and air as cladding layer.

3.2 Sol-gel process of film formation

The basis of SiO_2/Si technology is to deposit silica layers on silicon substrates, to define single-mode channel waveguides in this material, and to couple these guides to external fibers. In the absence of a taper or similar component, the mode fields of the channel guides should match those of single-mode silica fiber as closely as possible, in order to limit coupling losses. However, use of more strongly confining guides allows reduced bend radii and therefore lowers component size and also concentrates pump power, to great advantage in amplifiers and nonlinear devices [22]. The SiO_2-based glass layers can be easily deposited by spin coating using the sol-gel process. A two-step process based on the sol-gel process can be successful used for fabricating amorphous dielectric layers [21]:

1. formation of a stable suspension of particles within a liquid (the sol) and further processing of the sol to form mainly Si-O-Si bonds thought condensation reactions (aging sol);

2. spin-coating of the aging sol and rapid thermal annealing (multiple cycles) to form a thick and dense glassy film.

The first step involves the use of liquid metal alkoxide precursors of the desired glass composition. A common precursor for SiO_2 is tetraethoxysilane (TEOS), a liquid at room temperature insoluble in water but soluble in ethanol. This precursor

is hydrolyzed by addition of water to the solution, which allows condensation to begin to form the Si-O-Si bonds of the glass. However, other precursors may be used (added) following the same steps. For example, the process for preparation of SiO_2-TiO_2 solutions uses, for example, titanium isopropoxide IV (TPOT) as TiO_2 precursor [23]. After an aging time of ~16 h (**Figure 3**), the suspension is spun at typically 2500 rpm, during 30 s, upon which the solvent evaporates and the stages of solidification and drying are greatly accelerated for a few seconds, giving a thin layer of ~300 nm.

The gel must be heated to remove residual organics and to complete densification but this stage induces large tensile stresses [20–24]. The gel is therefore a three-dimensionally-linked solid network with liquid (solvents) filling the pores, which are interconnected in the wet gel state. The removal of solvent during drying proceeds simultaneously with condensation reactions and solidification. As the solvent is evaporated, a competing process leads to capillary pressure and the stresses induced by shrinkage increases. Thus, cracking may happen. It has been shown that the thickness of a single layer SiO_2 is limited to approximately 0.7 μm with the sol-gel method [25]. At thickness greater than 0.7 μm, the intrinsic stress and mismatch of thermal expansion coefficients between the sol-gel SiO_2 layer and the substrate causes cracks and peeling. Moreover, the constrained one-dimensional shrinkage due to the substrate creates tensile stress within the sol-gel layer [20–24], which must be annealed out to prevent cracking. Iteration of this process has been successful used to produce a multi-micron film [21]. Cracks and pores are almost inevitable in sol-gel derived films because of organic components, which must be eliminated during heat treatment. Thus, residual pores still remain in sol-gel waveguides after the removal of organic residues at high temperatures (**Figure 4**). By varying the precursor ratios in the sol, glasses of different composition, and thus refractive index, can be achieved; for example, SiO_2/TiO_2 of differing molar ratios allows a wide index range from 1.46 to over 1.6. In particular, for waveguide devices, a bilayer is formed: a lower index buffer (usually a SiO_2 layer), which must be sufficiently thick to prevent leakage of guided light into the substrate, and a higher index guiding layer (e.g., SiO_2-MO_2 (M = Ti, Zr, Hf) or SiO_2-HfO_2-MO_2 (M = Ti, Zr) materials [26]). The thickness and refractive index of films can be measured using a profilometer and an ellipsometer, respectively, as a function of the sol composition and preparation conditions (water, catalysts, and solvents amounts). The refractive index, whose control is necessary for the films to operate as planar waveguides in the SiO_2/Si technology, is usually tailored by doping the SiO_2 material, for example, with TiO_2 (or other, e.g., GeO_2). However, due to the

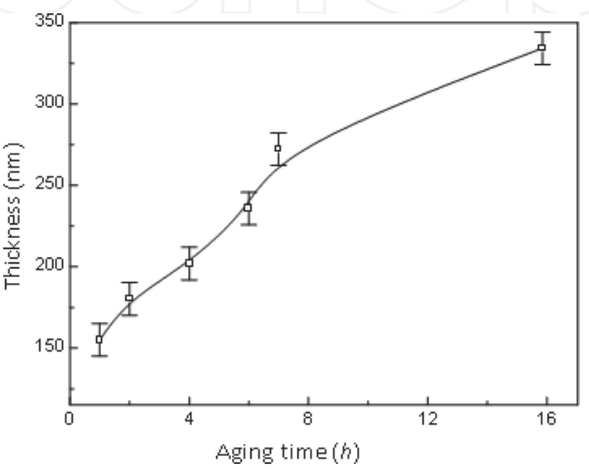

Figure 3.
Effect of aging time on the thickness of spin-coated sol-gel $90SiO_2$-$10TiO_2$ (mol%) films.

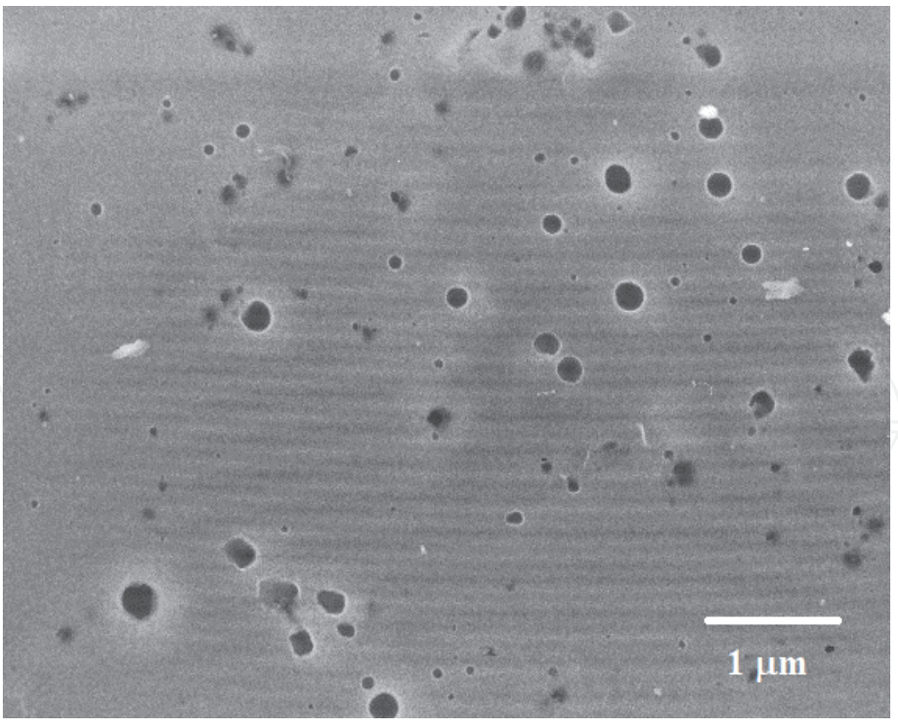

Figure 4.
A typical sol-gel glassy thin film. The dark circular regions represent the pores.

different rates of hydrolysis of the different precursor alkoxides, the compositional homogeneity of the derived material must be investigated by transmission electron microscopy (TEM) and Auger (or X-ray photoelectron spectroscopy (XPS)) analysis. It is also important to follow the evolution of the densification process through refractive index measurements but also directly measuring the surface area and porosity of the films after specific heat treatments, using the Brunauer-Emmett-Teller (BET) Surface Area Analysis and Barrett-Joyner-Halenda (BJH) Pore Size and Volume Analysis.

The guiding layers may also be doped with a functional material; for example, rare-earths (RE) can be added to the sol through a variety of precursors.

Also nonlinear properties can be introduced in silicate glasses by doping with semiconductor nanocrystals.

A modification of the most common planar bilayer guiding structure can be achieved by etching the layer of high index (n_2) into ridges (**Figure 5a**), which can then be melted (reflowed) to improve shape and surface quality and then buried under a top cladding glass (**Figure 5b**) of lower index (n_1). In an alternative approach, light can be guided in the high index layer by shallow ridges on the upper cladding layer; this is called a strip loaded structure (**Figure 5c**). In this case, etching and reflow at the guiding layer is avoided. The production of silica channel waveguides frequently employs photolithography; the mask for etching the strips can be the photoresist itself or a metallic film and reactive ion etching (RIE), which provides high anisotropy. Passive ridge waveguides were deposited on silicon by a solvent-assisted lithographic process incorporating simple mask technology and photosensitive sol-gel-derived glasses [27]. This approach uses direct writing of photosensitive glass with UV light.

With the synthesis of organic-inorganic films (ormosils), it is possible to obtain hybrid materials with film thickness much higher than 1 μm, which fit the requirements of optical waveguiding. For the preparation of these materials, TEOS (or other alkoxide) can be mixed together with organosilane polymers (e.g., polydimethylsiloxane (PDMS) or 3-(trimethoxysilyl)-propylmethacrylate

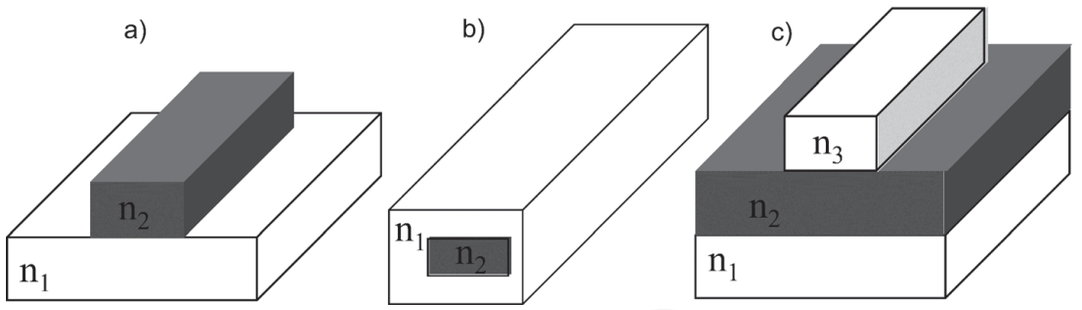

Figure 5.
Typical configuration of channel waveguides: (a) ridge waveguide, (b) buried waveguide, and (c) strip-loaded waveguide.

(TMSPM)), which keep trapped inside the oxide gel network during the hydrolysis and condensation reactions of TEOS [28]. In that case, the organic groups can further be used as oligomers since their backbone structures are similar to that of silica matrix. In addition, these groups can also improve physical, chemical, and mechanical properties of the hybrid materials, and the modification of inorganic network structures with organic groups allow the isomerization of organic photoactive molecules as compared to inorganic glasses [29]. It has been reported the use of two different silanes: γ-glycidyloxypropyltrimethoxysilane (GLYMO) and 3-(trimethoxysilyl)-propylmethacrylate (TMSPM) [30] for the preparation of TiO_2/ormosil waveguide films by the sol-gel method.

In view of the above discussion, it can be established that there are three main characteristics required for sol-gel waveguides:

1. mode shapes suitable for coupling to single-mode fibers (by absolute refractive index, refractive index difference and geometry);

2. compatibility with dopants (e.g., salts, alkoxides, organosilane polymers, etc.);

3. Compatibility with further processing steps, namely photonic materials with specific functional responses (e.g., optical amplification and nonlinear properties).

Some of the challenges still pending currently are: reduction of propagation losses for a planar waveguide to less than 1 dB/cm (although the short path lengths involved in integrated circuits make optical losses less of a problem), reduction coupling losses between optical fibers and integrated optical waveguides, and difficulty in directing light around sharp curves due to system miniaturization. Key future goals are to develop constituent functions required for fully integrated amplifiers; in particular, a tapered coupler for efficient power transfer between fibers and strong confinement guides, and a wavelength selective filter for coupling pump and signal wavelengths. A key issue is the need to achieve minimal loss with high confinement waveguides.

4. Doping silicate waveguides

4.1 Rare-earths doping for amplification

Optical fibers doped with rare-earth (RE) ions have contributed to the fast development of optical telecommunications [31]. Adding amplification to passive

functions of simple waveguides could allow low cost and compact amplifiers, through on chip integration of multiple components. Hence, developing RE-doped layers for optically pumped amplifiers is a key challenge. This can be provided in glasses doped with Nd^{3+} and Er^{3+}. Both have been widely used in fiber amplifiers and lasers, but in these cases, the gain was less important due to the very low losses in the fibers and the long path lengths that can easily be achieved.

In order to reduce the fiber and waveguide path lengths, the use of relatively large concentrations of RE ions of high quantum efficiency is required and, therefore owning long metastable level lifetimes. Nd^{3+} can be added to the sol as a nitrate and then converted to the oxide form by heat treatment. However, Nd_2O_3 is immiscible in silica glass for amounts higher than 0.5 wt% (by conventional melt-casting), and therefore it forms aggregates or clusters [32]. These clusters cause non-radiative deexcitation processes which greatly lower the fluorescence lifetime and thus the gain of the material. Hence, these lifetimes are seriously reduced by concentration quenching (or clustering) due to neighbor ion interactions in insufficient dilute systems. In addition, non-radiative quenching phenomena may also be caused by residual OH groups or by multiphonon relaxation, which are strongly favored in high vibrational energy matrices like silica glasses [33, 34]. Similar behavior is found for high levels of Er^{3+} ions in silicate glasses, also due to their poor solubility on that material. The ion dispersion is dependent on dopant concentration and on the solubility of dopant in the host material, which fortunately in the case of sol-gel glasses, can be improved. Hence, sol-gel-derived glasses are especially suitable to obtain homogenous compositions with a good dispersion of RE ions. Co-dopants (P_2O_5 or Al_2O_3) are often used to increase the solubility of the Er^{3+} doping. Er^{3+} is particularly interesting as it exhibits a laser transition at 1.55 μm and, thus, can provide amplification in the third optical communications window [31]. The energy-level structure of Er^{3+} allows pumping of the $^4I_{11/2}$ excited-state multiplet around 980 nm by semiconductor lasers and the $^4I_{13/2}$ excited-state multiplet is populated by subsequent multiphonon relaxation. Radiative relaxations of the $^4I_{13/2}$ to the $^4I_{15/2}$ ground-state multiplet may then provide gain near 1.55 μm [31].

However, the optical properties of RE-doped materials strongly depend on the host system, the dopant concentration, and the thermal background.

The method of incorporation of Er^{3+} consists in the dissolution of erbium salts (erbium (III) nitrate or chloride pentahydrate) into the sol, followed by aging and then coating. In this case, the ions will favor non-bridging oxygen sites in the gel as the solvent is evaporated. Introducing Er^{3+} in ionic form as dissolved salts is less effective for its incorporation into the sol network, and consequently, as the solvent is evaporated during film formation, some precipitation may occur, resulting in a segregated film. The use of an erbium alkoxide precursor favors the condensation reactions between the Er^{3+} ions and the host material in the sol and thus form a homogeneous structure with a strong possibility of avoid cracks formation during the densification process. In some cases, small amounts of TiO_2 or P_2O_5 nucleating agents are also added to the sol with the purpose of causing controlled nucleation and crystallization of erbium-containing nanocrystalites. This approach was successfully tested in the case of Er^{3+}:SiO_2-TiO_2 and Er^{3+}:SiO_2-TiO_2-P_2O_5 sol-gel glasses, where $Er_2Ti_2O_7$ and $ErPO_4$ nanocrystalline phases, respectively, with good spectroscopic properties, were obtained [35]. The precipitation of such nanocrystallites allows the control distribution of the Er^{3+} ion in the matrix, reducing their clustering effect and maximizing their quantum efficiency. To characterize the active properties of the waveguides, measurements of the fluorescence spectra and the lifetime of the erbium $^4I_{13/2}$ metastable level can be performed.

The surface structure (e.g., surface roughness, nanocrystallites, porosity, etc.) can be investigated by atomic force microscopy (AFM) and scanning electron

microscopy (SEM) (**Figure 4**). Clusters can be analyzed by grazing angle X-ray diffraction or very low frequency Raman scattering. To investigate the glass structure, it can be used X-ray absorption fine structure spectroscopy (EXAFS). This tool provides a good probe of RE nearest-neighbors and reveals, for example, where the Er^{3+} ions are well dispersed simple by Er-O bonds relative intensity [36]. A previous study reported from XPS analysis that Nd^{3+} may be incorporated in the P_2O_5 co-doped $80SiO_2$-$20TiO_2$ films at a higher concentration level than Er^{3+} in similar Al_2O_3 co-doped films [37]. Crystallization can, however, be investigated by X-ray diffraction (XRD) and crystal size can be estimated by the Scherrer equation. In particular, nanocrystallites are only seen at grazing incidence (0.4°), suggesting their main concentration at the surface [38]. In order to obtain concentration gradients through the total film thickness, Rutherford Backscattering Spectroscopy (RBS) can be used.

Fluorescence lifetime can be measured on multilayer planar waveguides, by launching diode laser pump light (796 nm for Nd^{3+}, 976 nm for Er^{3+}) into the cleaved input end of the waveguide. The fluorescence is collected at the output end and then focused onto a fast photodetector for further analyzes with a digital oscilloscope.

Since the formation of erbium containing nanocrystals in glass results in an increase for the 1.55 μm fluorescence (up to 9 ms) [35], the determination of characteristic temperatures such as glass transition (Tg), onset crystallization temperature (Tx), crystallization temperature (Tc), onset melting temperature (Txf), and melting temperature (Tf) is important in estimating the thermal stability of a glass and its susceptibility to temperature-induced changes during the film annealing. A study based on DTA analysis revealed that anatase crystallites appear as the primary crystalline phase in SiO_2-TiO_2-P_2O_5 glasses, while cristobalite precipitates near 1000°C [39]. Thus, the characterization of these temperatures using differential thermal analysis (DTA) technique would be a great help to define the thermal treatment of the sol-gel glasses derived waveguides.

4.2 Semiconductor microcrystallites doping for nonlinear optics

Semiconductor quantum dots dopants (Cds, Pbs) can extend the functionality of passive glassy waveguides toward possible applications in nonlinear guided wave devices (nonlinear directional coupler, Mach-Zehnder interferometer). Significant enhancement of $\chi(3\omega)$ due to quantum confinement has been demonstrated in glass doped with CdS_xSe_{1-x} and CuCl microcrystals [40]. In both cases, the large band gap means that the non-linearity can only be exploited at visible or near-UV. Recently, narrow-gap dopants have been fabricated at near-IR wavelengths [41].

Two main routes have been followed in the development of such materials, namely the addition and reaction of the dopants inside the initial sol-gel solution, by chemically controlling the size of the particles (sol-doping), and the impregnation or exposition of a nanoporous sol-gel film to the dopants (pore doping), where the crystal size is limited by the pore size. The pore doping has been successfully applied for over 20 years [42] to prepare films for integrated optics applications. In the sol doping, $Cd(NO_3)_2$ and $Pb(NO_3)_2$ is mixed in aqueous solution since both nitrates have very high solubilities and the resulting solution absorbed into a dry porous SiO_2 layer. The excess liquid is then spun off and a flux of H_2Te gas is forced to pass over the layer in order to achieve, for example, Cd1-xPbxTe microcrystallites. Otherwise, if the intention is rather precipitate CdS or PbS, H_2S can be used as reactive gas. The samples are then dried in vacuum and properly annealed. To prove the existence of microcrystallites precipitates, TEM and grazing incidence XRD is often employed to verify their presence in the host glass. Moreover,

semiconductor microcrystallites are known to exhibit an absorption edge blue shifted (toward shorter wavelength) with respect to the bulk semiconductor. This shift is a typical behavior of microcrystallites that can be analyzed by UV-visible absorption spectroscopy in order to calculate their quantum size [42]. Finally, the Z-scan technique is a popular method for testing optical nonlinearities of bulk materials, namely the non-linear index n_2 (Kerr coefficient) and the non-linear absorption coefficient $\Delta\alpha$. However, these techniques are inappropriate for nonlinear measurements in planar optical waveguides due to its low thickness. Therefore, nonlinear m-line spectroscopy is a suitable alternative based on the analysis of the nonlinear change in the shape of the dark line associated with the excitation of guided waves [43]. This is an easy technique for the determination of Kerr properties of thin films, which are the basis of optical waveguides [43]. The third-order optical nonlinearity (Kerr effect) of CsS-doped SiO_2/Si planar waveguide was measured using an m-line technique, yielding a value of -5×10^{-9} cm^2/kW [44].

5. Conclusions

Silica glass (by sol-gel synthesis) is one of the most widely used materials in the production of optical waveguides, due to its many advantages (versatility, low cost manufacturing, chemical resistance, and low synthesis temperature). The chemical kinetics of the conversion reaction of TEOS to SiO_2 (or other glass compositions) is very sensitive to the physical and chemical parameters of the process (e.g., water content, type of catalyst, and aging). However, its versatility is one of its main advantages because allows the production of a diversity of compositions and structures. The spin-coating process allows homogeneous and thick films to be deposited, which perfectly match the physical requirements of planar optical waveguides and that of SiO_2/Si technology. However, silicate glasses exhibit some disadvantages, such as high phonon energy and low luminescent ion solubility, which affect the quantum efficiency or luminescent ion emission bandwidth. Therefore, some strategies must be taken to improve their optical behavior. In fact, by slightly modifying the composition of the silica glass, we are able to control the refractive index and achieve not only passive waveguides but also the active ones, with tailored properties to many applications. Moreover, it is also possible to take advantage of the pores in order to optimize the precipitation of semiconductor microparticles and benefit of all the linear and nonlinear features of optical devices. Nowadays, the requirements for photonic components in communication systems have increased and become more demanding. While other technologies have made constant improvements, the potential advantages of the sol-gel approach remain valid and have now been plainly demonstrated. Although many of the procedures implemented are more than 25 years old, it is certain that, without all these fundamentals, the present development in the field of optical waveguides would not be the same.

Author details

Helena Cristina Vasconcelos[1,2]

1 Faculty of Sciences and Technology, Azores University, Ponta Delgada, Portugal

2 Faculty of Science and Technology, Department of Physics, Centre of Physics and Technological Research (CEFITEC), New University of Lisbon, Caparica, Portugal

*Address all correspondence to: helena.cs.vasconcelos@uac.pt

References

[1] Wilson J, Hawkes JFB. Optoelectronics: An Introduction. Taipei, Taiwan: Pearson Education Taiwan Ltd; 2010

[2] Miller SE. Integrated optics: An introduction. Bell System Technical Journal. 1969;**48**:2059-2069. DOI: 10.1002/j.1538-7305.1969.tb01165.x

[3] Osterberg H, Smith LW. Transmission of optical energy along surfaces: Part II, inhomogeneous media. Journal of the Optical Society of America. 1964;**54**:1078-1084. DOI: 10.1364/JOSA.54.001078

[4] Boyd RW. Nonlinear Optics. 3rd ed. USA: Academic Press, Inc.; 2008

[5] Yeatman EM. Sol-gel fabrication for optical communication components: Prospects and progress, In: Proc. SPIE. 1997;**68**:119. DOI: 10.1117/12.279834

[6] MacCraith BD, McDonagh C, McEvoy AK, Butler T, O'Keeffe G, Murphy V. Optical chemical sensors based on sol-gel materials: Recent advances and critical issues. Journal of Sol-Gel Science and Technology. 1997;**8** (1053). DOI: 10.1023/A:1018338426081

[7] Marcuse D. Chapter 1 - The Asymmetric Slab Waveguide. In: Marcuse D, editor. Theory of Dielectric Optical Waveguides. 2nd ed. Academic Press; 1991. pp. 1-59. DOI: 10.1016/B978-0-12-470951-5.50007-X

[8] Grivas C. Optically pumped planar waveguide lasers, part I: Fundamentals and fabrication techniques. Progress in Quantum Electronics. 2011;**35**(6): 159-239. DOI: 10.1016/j.pquantelec.2011.05.002

[9] Okamoto K. Fundamentals of Optical Waveguides. San Diego: Academic Press; 2000

[10] Wild WJ, Giles CL. Goos-Hänchen shifts from absorbing media. Physical Review A. 1982;**25**(4):2099-2101

[11] Hunsperger RG. Integrated Optics: Theory and Technology. 6th. ed. Springer Publishing Company, Incorporated; 2009

[12] Righini GC, Klein L, et al., editors. Handbook of sol-gel science and technology. In: Characterization of Sol–Gel Thin-Film Waveguides. DOI: 10.1007/978-3-319-19454-7_46-1

[13] Yeatman EM. Thin-film optical waveguides. In: Aegerter MA, Mennig M, editors. Sol-Gel Technologies for Glass Producers and Users. Boston, MA: Springer; 2004. DOI: 10.1007/978-0-387-88953-5_42

[14] Yoshiki W, Tanabe T. All-optical switching using Kerr effect in a silica toroid microcavity. Optics Express. 2014;**22**:24332-24341

[15] Semiconductor Quantum Dots, Bányai L, Koch SW. World Scientific Series on Atomic, Molecular and Optical Physics; 1993

[16] Silica-on-Silicon Integrated Optics. Available from: http://www3.imperial.ac.uk/pls/portallive/docs/1/2475919.PDF

[17] Giancarlo C, Righini AC. Glass optical waveguides: A review of fabrication techniques. Optical Engineering. 2014;**53**(7):071819. DOI: 10.1117/1.OE.53.7.071819

[18] Esposito S. "Traditional" Sol-gel chemistry as a powerful tool for the preparation of supported metal and metal oxide catalysts. Materials. 2019;**12**(4):668. DOI: 10.3390/ma12040668

[19] Biswas PK. Journal of Sol-Gel Science and Technology. 2011;**59**:456. DOI: 10.1007/s10971-010-2368-5

[20] Ho C, Ngo QN, Pita K. Understanding the Cause of Cracking in Sol-Gel-Derived Films. 2007. DOI: 10.13140/RG.2.1.4084.8724

[21] Hill C, Jones S, Boys D. Rapid thermal annealing - theory and practice. In: Levy RA, editor. Reduced Thermal Processing for ULSI. Nato asi Series (Series B: Physics). Vol. 207. Boston, MA: Springer; 1989

[22] Selvaraja SK, Sethi P. Review on optical waveguides. In: You KY, editor. Emerging Waveguide Technology. IntechOpen; 2018. DOI: 10.5772/intechopen.77150. Available from: https://www.intechopen.com/books/emerging-waveguide-technology/review-on-optical-waveguides

[23] Orignac X, Vasconcelos H, Du X, et al. Journal of Sol-Gel Science and Technology. 1997;**8**:243. DOI: 10.1023/A:1026497826255

[24] Guozhong C, Ying W. Nanostructures and Nanomaterials: Synthesis, Properties, and Applications

[25] Langlet M. Low-temperature processing of sol–gel thin films in the SiO_2–TiO_2 binary system. In: Klein L, Aparicio M, Jitianu A, editors. Handbook of sol-Gel Science and Technology. Cham: Springer; 2017. DOI: https://doi.org/10.1007/978-3-319-19454-7_15-1

[26] Marques AC, Almeida RM. Raman spectra and structure of multicomponent oxide planar waveguides prepared by sol-gel. Journal of Sol-Gel Science and Technology. 2006;**40**:371-378. DOI: 10.1007/s10971-006-9320-

[27] Fardad A, Andrews M, Milova G, Malek-Tabrizi A, Najafi I. Fabrication of ridge waveguides: A new solgel route. Applied Optics. 1998;**37**:2429-2434

[28] Mackenzie JD. Journal of Sol-Gel Science and Technology. 1994;**2**:81. DOI: 10.1007/BF00486217

[29] Zhang X, Xue C, Zhang W, Yu L, Wang Q, Que W, et al. Multifunctional TiO_2/ormosils organic-inorganic hybrid films derived by a sol-gel process for photonics and UV nanoimprint applications. Optical Materials Express. 2019;**9**:304-314

[30] Wang B. Optical and surface properties of hybrid TiO_2/ormosil planar waveguide prepared by the sol–gel process. Ceramics International. 2006;**32**:7-12. DOI: 10.1016/j.ceramint.2004.11.013

[31] Desurvire E, Bayart D, Desthieux B, Bigo S. Erbium Doped Fiber Amplifiers: Device and System Developments. Wiley Interscience; 2002. ISBN: 0-471-41903-6

[32] Natarajan S, Ramamurthi A, Selvarajan A, Muthuraman M, Patil K. Amplification of Light in Sol-Gel-Based Nd-Glass Waveguides; 1998

[33] Vasconcelos H, Pinto A. Fluorescence Properties of Rare-Earth-Doped sol-Gel Glasses. 2017. DOI: 10.5772/intechopen.68534

[34] Vasconcelos HC, Pinto AS. Rare-earth activated glasses in integrated optical devices with different geometric shapes: Fibers, planar waveguides and microspheres. In: Photoluminescence: Advances in Research and Applications. Nova Science Publishers, Inc.; 2018. pp. 53-96

[35] Strohhöfer C, Fick J, Vasconcelos HC, Almeida R. Active optical properties of Er-containing crystallites in sol–gel derived glass films. Journal of Non-Crystalline Solids. 1998;

226:182-191. DOI: 10.1016/S0022-3093(98)00365-2

[36] Santos L, Vasconcelos H, Marques M, Almeida R. Active nanocrystals in erbium-doped silica-titania sol-gel films. Materials Science Forum. 2004;**455–456**:545-549. DOI: 10.4028/www.scientific.net/MSF.455-456.545

[37] Almeida R, Vasconcelos H, Gonçalves MC, Santos L. XPS and NEXAFS studies of rare-earth doped amorphous sol–gel films. Journal of Non-Crystalline Solids. 1998;**232**:65-71. DOI: 10.1016/S0022-3093(98)00545-6

[38] Almeida RM, Vasconcelos HC. Rare-earth doped nanocrystals in planar waveguides. In: Fundamentals of Glass Science and Technology. Vaxjo, Sweden: Glafo, the Glass Research Institute; 1997. pp. 110-117

[39] Vasconcelos H. The effect of PO2,5 and AlO1,5 additions on structural changes and crystallization behavior of SiO_2-TiO_2 sol-gel derived glasses and thin films. Journal of Sol-Gel Science and Technology. 2010;**55**. DOI: 10.1007/s10971-010-2223-8

[40] Zimin LG, Gaponenko SV, Lebed VY, Malinovskii IE, Germanenko IN. Nonlinear optical absorption of CuCl and CdS_xSe_{1-x} microcrystallites under quantum confinement. Journal of Luminescence. 1990;**46**(2):101-107. DOI: 10.1016/0022-2313(90)90012-z

[41] Kovalenko M, Heiss W, Shevchenko E, Lee J-S, Schwinghammer H, Alivisatos, et al. SnTe Nanocrystals: A new example of narrow-gap semiconductor quantum dots. Journal of the American Chemical Society. 2007;**129**:11354-11355. DOI: 10.1021/ja074481z

[42] Dawnay EJC, Fardad MA, Green M, Horowitz F, Yeatman EM, Almeida RM, et al. In: Vincenzini P, Righini GC, editors. Advanced Materials in Optics, Electro-Optics and Communication Technologies. Faenza, Italy: Techna; 1995. pp. 55-62

[43] Kajzar F. M-line spectroscopy for nonlinear characterization of polymeric waveguides. Optical Engineering. 1995;**34**(12):3418. DOI: 10.1117/12.213240

[44] Fardad MA, Fick J, Green M, Guntau M, Yeatman EM, Vitrant G, et al. Fabrication and characterisation of a CdS-doped silica-on-silicon planar waveguide. IEE Proceedings - Optoelectronics. 1996;**143**(5):298-302. DOI: 10.1049/ip-opt:19960836